Tensor-Based DOA Estimation for Array Virtual Translation

Jiaqiang Peng
Air Force Engineering University
Guimei Zheng (zheng-gm@163.com)
Air Force Engineering University https://orcid.org/0000-0001-9779-6014

Research

Keywords: Tensor decomposition, Array virtual translation, DOA estimation, Array aperture

Posted Date: September 8th, 2021

DOI: https://doi.org/10.21203/rs.3.rs-842179/v1

RESEARCH

Tensor-Based DOA Estimation for Array Virtual Translation

Jiaqiang Peng and Guimei Zheng*

*Correspondence:
zheng-gm@163.com
Air Force Engineering University, Xi'an, China
Full list of author information is available at the end of the article

Abstract

In order to make up for the problem that the tensor-based spatial smoothing DOA estimation algorithm cannot make good use of the physical aperture of the array, this paper proposes a tensor-based array virtual translation DOA estimation algorithm. Under the framework of the tensor-based DOA estimation algorithm, the algorithm applies the array virtual translation technique to the factor matrix obtained after tensor decomposition, which can be expanded into signal subspace and approximately has a Vandermonde structure. Furthermore, the available array aperture of the algorithm is expanded, the estimation accuracy is improved, and the limitation of the physical array aperture on the algorithm's multi-target estimation ability is broken. Since the processing technique proposed in this paper has nothing to do with the construction of tensors, this technique is suitable for all DOA estimation algorithms based on tensors. Theoretical analysis and numerical simulation verify the effectiveness of the algorithm proposed in this paper.

Keywords: Tensor decomposition; Array virtual translation; DOA estimation; Array aperture

1 Introduction

Direction of arrival(DOA) estimation has always been an important part and hot research object in the field of radar signal processing, and is widely used in sonar, wireless communication and other fields. After more than a century of development, with the enthusiasm of many scholars, very fruitful theoretical results have been produced. Among them, the most famous ones are multiple signal classification(MUSIC)[1] and estimation of signal parameters via rotational invariance techniques(ESPRIT)[2]. The subspace-based algorithm represented by the two algorithms has a good estimate performance when the number of snapshots is sufficient, the signal is incoherent, and the signal-to-noise ratio(SNR) is high. Once one of the above conditions is not established, the estimation performance will be greatly reduced, or even the estimation will be invalid. In order to solve the problem of coherent target estimation, the spatial smoothing algorithm [3, 4, 5, 6] came into being. The algorithm sacrifices the array aperture for the estimation ability of coherent targets. Therefore, its estimation ability of multiple targets and estimation accuracy are reduced. The maximum likelihood estimation algorithm [7, 8] provides a solution for DOA estimation in small snapshot and low SNR scenes, but it can not be accepted by many applications because of its large amount of calculation. Although the DOA estimation algorithm based on compressed sensing [9, 10, 11, 12] can be applied to complex scenes such as small snapshots, low SNR, and missing

elements, it is extremely inefficient in high-dimensional data processing. Moreover, due to its inherent requirements for data sparsity, the number of estimable targets is less under a certain number of elements [13]. However, the newly emerged tensor-based DOA estimation algorithm is favored by many scholars because of its ability to efficiently process high-dimensional data, strong denoising ability, and being applicable to single snapshot and multiple snapshots [14, 15, 16, 17, 18, 19, 20]. Under certain conditions such as SNR and number of snapshots, this kind of algorithm can decompose the approximately pure steering vector matrix as the factor matrix of the estimation tensor model by using the low rank characteristics and internal structure of the received signal data, and then obtain the DOA information of the target by using the rotation invariance characteristics of Vandermonde matrix or other subspace-based DOA estimation algorithms. It is easy to see that this kind of algorithm has strong structural characteristics, and its key point is how to decompose the steering vector information of the signal as the factor matrix of the tensor. In the tensor-based single snapshot or one-dimensional DOA estimation problem, the idea of spatial smoothing is mainly adopted to smooth the received data into overlapping sub matrices, and then stack the sub matrices in a certain dimension of the tensor to form an estimation tensor model [15, 16]. Similar to the traditional spatial smoothing DOA estimation algorithm, the array aperture of the factor matrix decomposed by the estimation tensor model formed by this construction method is the physical array aperture of the sub array. Therefore, using this factor matrix to extract the target DOA information will reduce the target estimable number and degrade the estimation accuracy due to the loss of array aperture. Can the array aperture of the factor matrix expanded into the signal subspace be restored to the physical aperture of the original array or even exceed the physical aperture of the original array through a certain processing technology? This paper gives an affirmative answer.

Inspired by the aforementioned question, this paper proposes an array virtual translation DOA estimation algorithm based on tensor. Under the framework of the DOA estimation algorithm based on tensor, this algorithm applies the array virtual translation technology to the factor matrix that can be expanded into signal subspace, so that the processed data is expanded by nearly double the array aperture of the original data, and the estimation accuracy of the algorithm and the number of estimable targets are greatly improved. However, the processing procedure has nothing to do with the way the tensor is constructed. Therefore, this processing technique is applicable to all DOA estimation algorithms based on tensor. Theoretical analysis and numerical simulation experiments have verified its feasibility and ease of use.

The rest of the paper is arranged as follows: the second part describes the algorithm proposed in this article in detail; the third part gives the analysis and simulation results of the algorithm proposed in this paper in the application of DOA estimation; finally, the full text is summarized.

Notations: The caligraphic letter $\mathcal{A}$ represents a tensor, the uppercase bold Italian letter $\boldsymbol{A}$ represents a matrix, the lowercase bold Italian letter $\boldsymbol{a}$ represents a vector, the superscript $(\bullet)^T, (\bullet)^*, (\bullet)^H$ represents transpose, conjugation and conjugate transpose respectively, $\mathbb{C}$ represents the set of complex numbers, $\mathbb{R}$ represents

the set of real numbers, $\mathcal{H}$ represents Hank operator, $diag(\bullet)$ means diagonal transformation, that is, when the object in brackets is a vector, it will form a diagonal matrix, when the diagonal in the brackets is a matrix, the diagonal elements of the matrix are taken to form a vector, $vec(\bullet)$ represents vectorization operation, $\odot$ represents the KhatriRao product, $inv(\bullet)$ represents the inversion operation, $\dagger$ represents the generalized inverse operation, *asind* represents the inverse trigonometric function, $\lceil\bullet\rceil$ represents round up, $\circ$ represents the tensor product, $\mathcal{T}_{[i]}$ represents mode-i matricization of $\mathcal{T}$. The elements in vectors, matrices, and tensors, row vectors or column vectors in matrices, and fibers and slices in tensors are all adopt the representation method in MATLAB. In the element index, *end* represents the last index value.

2 Methods

2.1 Basic principle of DOA estimation algorithm based on tensor

In the DOA estimation algorithm based on tensor, it is first necessary to perform some transformation on the received data in order to decompose the steering vector information as a factor matrix of the tensor. Take the construction of a third-order estimated tensor model in a noise-free environment as an example. Normally, the data needs to be transformed into the following form,

$$\boldsymbol{X}_i = \boldsymbol{A} diag\left(\boldsymbol{D}(:,i)\right)\boldsymbol{B}^T \tag{1}$$

where $\boldsymbol{A}$ and $\boldsymbol{B}$ are the matrices containing the steering vector information. $\boldsymbol{D}(:,i)$ is the target's i-th snapshot signal or the i-th pulse reflection cross-sectional area(RCS). Taking $\boldsymbol{X}_i$ as a slice in the third dimension of the tensor and stacking successive snapshots or successive pulses can form the following estimated data model.

$$\mathcal{T}(:,:,i) = \boldsymbol{X}_i \tag{2}$$

$$\mathcal{T}_{[1]} = \boldsymbol{B}\left(\boldsymbol{A}\odot\boldsymbol{D}^T\right)^T \tag{3}$$

$$\mathcal{T}_{[2]} = \boldsymbol{A}\left(\boldsymbol{D}^T\odot\boldsymbol{B}\right)^T \tag{4}$$

$$\mathcal{T}_{[3]} = \boldsymbol{D}^T\left(\boldsymbol{A}\odot\boldsymbol{B}\right)^T \tag{5}$$

$$\mathcal{T} \approx [[\boldsymbol{B},\boldsymbol{A},\boldsymbol{D}]] \equiv \sum_{r=1}^{K}\boldsymbol{B}(:,r)\circ\boldsymbol{A}(:,r)\circ\boldsymbol{D}^T(:,r) \tag{6}$$

Carrying out canonical polyadic decomposition(CPD) or higher-order singular value decomposition(HOSVD) on $\mathcal{T}$ can get matrices $\boldsymbol{E}$ and $\boldsymbol{F}$ that can be expanded into the same signal subspace as $\boldsymbol{A}$ and $\boldsymbol{B}$. Thanks to the high denoising performance of the tensor CPD under certain conditions, the matrices $\boldsymbol{E}$ and $\boldsymbol{F}$ will better maintain the Vandermonde structure, so we can take advantage of its rotation invariance

characteristics or other DOA subspace-based estimation algorithm to obtain the DOA information of the target.

Remark 1: It is assumed that each operation in the above expression meets the dimensionality requirements of the data. For the sake of simplicity, the above expressions are all formal expressions, omitting the dimensional information and deep structure information of the data. Among them, the matrixes $\boldsymbol{A}$ and $\boldsymbol{B}$ containing steering vector information can be one-dimensional steering vector matrices, corresponding to third-order tensors, or multi-dimensional steering vector matrices corresponding to higher-order tensor. But through decomposition, a factor matrix containing only one-dimensional steering vector information can be obtained. This paper will use CPD to calculate tensors, so here is mainly a list of tensor expressions related to CPD. For other expressions of tensors and their corresponding calculation methods, please refer to [21, 22, 23].

2.2 The proposed algorithm

According to the principle explained in the section 2.1, assuming that the matrix $\boldsymbol{E} \in \mathbb{C}^{N\times K}$ is a factor matrix containing one-dimensional steering vector information after CPD. In order to ensure that the matrix still has an approximate Vandermonde structure after the virtual translation processing of the array receive data, we first divide the matrix $\boldsymbol{E}$ by itself first row to get the normalized matrix $\tilde{\boldsymbol{E}}$, that is

$$\tilde{\boldsymbol{E}} = \boldsymbol{E}./\boldsymbol{E}(1,:) \tag{7}$$

and then perform array symmetric virtual translation processing on the matrix $\tilde{\boldsymbol{E}}$, namely

$$\boldsymbol{Y} = \left[\tilde{\boldsymbol{E}}^{*}\left(end:-1:2,:\right);\tilde{\boldsymbol{E}}\right] \tag{8}$$

Equation (8) clearly shows that the array aperture of $\boldsymbol{Y}$ is 2N-1. Since the matrix $\boldsymbol{Y}$ approximately has a Vandermonde structure, the following formula uses its rotation invariance feature to extract the DOA information of the target, let

$$\boldsymbol{Y}_1 = \boldsymbol{Y}(1:end-1,:) \tag{9}$$

$$\boldsymbol{Y}_2 = \boldsymbol{Y}(2:end,:) \tag{10}$$

According to the principle of ESPRIT algorithm [2], it is easy to kown that the matrix $\boldsymbol{Y}_1$ and $\boldsymbol{Y}_2$ have the following relationship

$$\boldsymbol{Y}_2 = \Psi\,\boldsymbol{Y}_1 \tag{11}$$

$$\Psi = \boldsymbol{Y}_1^{\dagger}\,\boldsymbol{Y}_2 = inv\left(\boldsymbol{Y}_1^{H}\,\boldsymbol{Y}_1\right)\,\boldsymbol{Y}_1^{H}\,\boldsymbol{Y}_2 \tag{12}$$

where Ψ is the diagonal matrix containing the DOA information of the target, and each diagonal element corresponds to one DOA information. Let θ_i represents the

i-th angle, and its value range is determined according to a specific scene. In the case of a half-wavelength between the array elements, each DOA information can be obtained by the following formula

$$\theta_i = asind\left(log\left(-i\Phi_{ii}/pi\right)\right) \tag{13}$$

3 Results and Discussion

3.1 Application examples

In order to show the general applicability of the proposed algorithm in this paper, the following are the examples of its application in one-dimensional and two-dimensional DOA estimation problems.

3.1.1 One-dimensional DOA estimation

For a uniform linear array with a half-wavelength array element spacing, assuming that the number of elements is N and the number of targets is K, the data obtained after L snapshot sampling can be expressed as

$$\boldsymbol{X} = \boldsymbol{A}\boldsymbol{S} + \boldsymbol{W} \tag{14}$$

$$\boldsymbol{A} = \left[\boldsymbol{a}_1, \cdots, \boldsymbol{a}_K\right] \tag{15}$$

$$\boldsymbol{a}_i = \left[1, \exp\left(j\pi sind\left(\theta_i\right)\right), \ldots, \exp\left(j\pi\left(N-1\right)sind\left(\theta_i\right)\right)\right]^T \tag{16}$$

where $\boldsymbol{A} \in \mathbb{C}^{N\times K}$ represents the steering vector matrix, $\boldsymbol{a}_i \in \mathbb{C}^{N\times 1}$ represents the steering vector of the i-th target, $\boldsymbol{S} \in \mathbb{C}^{K\times L}$ represents the received echo signal, $\boldsymbol{W} \in \mathbb{C}^{N\times L}$ represents independent and identically distributed Gaussian white noise.

In order to use the tensor-based DOA estimation algorithm, we hankize the received single snapshot data to form a Hank matrix and use it as a frontal slice on the third dimension of the third-order tensor to stack snapshots one by one to form an estimated tensor data model. The construction dimension is set as $n_1 = \lceil \frac{N+1}{2} \rceil$, $n_2 = N + 1 - n_1$, the specific expression is as follows:

$$\begin{aligned}\mathcal{H}\boldsymbol{X}(:,i) &= \begin{bmatrix} \boldsymbol{X}(1,i) & \boldsymbol{X}(2,i) & \cdots & \boldsymbol{X}(n2,i) \\ \boldsymbol{X}(2,i) & \boldsymbol{X}(3,i) & \cdots & \boldsymbol{X}(n2+1,i) \\ \vdots & \vdots & \ddots & \vdots \\ \boldsymbol{X}(n1,i) & \boldsymbol{X}(n1+1,i) & \cdots & \boldsymbol{X}(N,i) \end{bmatrix} \\ &= \boldsymbol{A}\left(1:n_1,:\right) diag\left(\boldsymbol{S}(:,i)\right) \boldsymbol{A}^H\left(1:n_2,:\right)\end{aligned} \tag{17}$$

$$\mathcal{T}\left(:,:,i\right) = \mathcal{H}\boldsymbol{X}(:,i) \tag{18}$$

Use the cpd_nls program in the Tensorlab toolbox [24] to perform CPD on $\mathcal{T}$ to get factor matrix $\boldsymbol{U}_1 \in \mathbb{C}^{n_1\times K}$ and $\boldsymbol{U}_2 \in \mathbb{C}^{n_2\times K}$ which are similar to matrices $\boldsymbol{A}\left(1:n_1,:\right)$ and $\boldsymbol{A}\left(1:n_1,:\right)$ respectively. When N is an odd number, it is easy to know that $n_1 = n_2$, then the array aperture can be restored to the original physical array aperture N when using the algorithm proposed in this paper to extract the target DOA information, no matter use $\boldsymbol{U}_1$ or $\boldsymbol{U}_2$; When N is an even number, it

is easy to know that $n_1 = n_2 + 1$, then if we use $\boldsymbol{U}_1$ to extract the target DOA information, the available array aperture is N+1, and if we use $\boldsymbol{U}_2$ to extracts the target DOA information, the available array aperture is N-1. In practical application scenarios, we can choose the construction dimension of the Hank matrix as appropriate to obtain a larger array aperture expansion. For example, the number of elements in one dimension is only one more than the number of targets, and the factor matrix of the other dimension is used for data processing when extracting the DOA information of the target.

Remark 2: For the one-dimensional DOA estimation algorithm based on tensor, the construction method of the tensor estimation model based on the Hank matrix and the construction method of the tensor estimation model using the spatial smoothing idea are essentially the same [15, 16]. The former is mainly used here to facilitate readers' understanding.

3.1.2 Two-dimensional DOA estimation

Assuming that the array is a uniform rectangular array, the spacing between the array elements is half a wavelength, the target number is K, and the number of array elements in the two dimensions are N and M respectively, then the single pulse data received after matched filtering and other processing can be expressed as

$$\boldsymbol{X}_i = \boldsymbol{A} diag\left(\boldsymbol{D}\left(:, i\right)\right) \boldsymbol{B}^T + \boldsymbol{W}_i \tag{19}$$

where $\boldsymbol{X}_i \in \mathbb{C}^{N \times M}$ is the i-th pulse echo data, $\boldsymbol{A} \in \mathbb{C}^{N \times K}$ and $\boldsymbol{B} \in \mathbb{C}^{M \times K}$ are the steering vector matrices corresponding to the two dimensions, respectively. Its definition is similar to formula (15), so it will not be explained in detail here. $\boldsymbol{W}_i \in \mathbb{C}^{N \times M}$ is independent and identically distributed Gaussian white noise. Similarly, stacking $\boldsymbol{X}_i$ as a frontal slice in the third dimension of the third-order tensor pulse by pulse can form a tensor estimation model, namely

$$\mathcal{T}\left(:, :, i\right) = \boldsymbol{X}_i \tag{20}$$

Use the cpd_nls program in the Tensorlab toolbox to perform CPD on $\mathcal{T}$ can obtain the factor matrix $\boldsymbol{U}_1 \in \mathbb{C}^{N \times K}$ and $\boldsymbol{U}_2 \in \mathbb{C}^{M \times K}$, which are similar to the matrix $\boldsymbol{A}$ and $\boldsymbol{B}$. When the algorithm proposed in this paper uses $\boldsymbol{U}_1$ and $\boldsymbol{U}_2$ to extract the two-dimensional DOA information of the target, it can correspondingly expand the array aperture to 2N-1 and 2M-1, which is approximately 2 times the aperture of the original physical array. After obtaining the two-dimensional DOA information, the final two-dimensional DOA information can be obtained by using the mature matching technology. Since the focus of this paper is on the expansion of the array aperture, the problems related to pairing are omitted here.

3.2 Numerical simulation

This section conducts a numerical simulation experiment on the DOA estimation problem described in Section 3.1. Unless otherwise specified, the simulation parameters are executed in accordance with Table 1. In the experiment, the tensor-based

DOA estimation algorithm uses the least squares ESPRIT technique to extract the DOA information after obtaining the factor matrix which containing the steering vector information, and compares and analyzes the DOA estimate performance with the standard one-dimensional or two-dimensional ESPRIT algorithm. For the convenience of subsequent description, we collectively refer to the conventional one-dimensional and two-dimensional tensor-based DOA estimation algorithm as tensor-based algorithms, and collectively refer to the one-dimensional and two-dimensional ESPRIT algorithm as the ESPRIT algorithm. The specific dimensions of this algorithm can be easily judged by the context.

3.2.1 One-dimensional DOA estimation

In the experiments in this section, the tensor-based algorithm and the algorithm proposed in this paper are both using tensor data $\mathcal{T}$ to extract the DOA information of the target, while the ESPRIT algorithm uses matrix data X to extract the DOA information of the target.

3.2.1.1 Comparison of estimation performance under different target numbers

In this experiment, we compared and analyzed the root-mean-square error(RMSE) values of the corresponding algorithm when the number of targets to be estimated varies from 3 to 6. At the same time, in order to further explore the estimation performance of the algorithm poposed in this paper, we also compared the estimated accuracy at 5 targets $DOAs = [10°, 20°, 30°, 40°, 50°]$. The experimental results are shown in Figure 1 to Figure 3.

From a theoretical point of view, when the number of array elements is 7, the array aperture of the factor matrix which containing steering vector information and obtained by the tensor-based algorithm is 4, which can estimate the DOA information of 3 targets at most. When the number of estimated targets exceeds 3, the estimation performance will be degraded. And the available array aperture of ESPRIT algorithm and the algorithm poposed in this paper are both 7, so they can estimate DOA information of 6 targets at most, but due to the influence of factors such as noise and the number of snapshots, this theoretical value cannot be achieved in practice. From the simulation results, Figure 1 shows that the RMSE of the three algorithms increases with the increase of the number of targets. And the error curve of the algorithm poposed in this paper and the ESPRIT algorithm is better than that of the tensor-based algorithm because the available array aperture of the tensor-based algorithm is relatively small. When the number of targets is 3, the three algorithms can achieve higher estimation accuracy. Among them, the error of the algorithm poposed in this paper is less than that of the ESPRIT algorithm, and the error of the ESPRIT algorithm is less than that of the tensor-based algorithm, which shows that under the same estimation conditions, DOA estimation algorithm based on tensor has better estimation accuracy than ESPRIT algorithm. However, when the number of targets is greater than or equal to 4, although the estimation accuracy of the algorithm poposed in this paper is significantly higher than that of the tensor-based algorithm, it is worse than the estimation accuracy of the ESPRIT algorithm. This is because although the available array aperture of the algorithm poposed in this paper is the same as the ESPRIT algorithm, its data

is derived from the tensor-based algorithm which only contains 4 array aperture information, so the amount of information available is nearly half less than that of the ESPRIT algorithm. The angle estimation problem in Figure 2 also shows that the tensor-based algorithm completely fails when estimating the 5 targets, and the estimation accuracy of the algorithm poposed in this paper is lower than that of the ESPRIT algorithm. In order to verify that the algorithm poposed in this paper can make up for this deficiency by expanding the aperture of the array, in the experiment shown in Figure 3, we changed the dimension of the Hank matrix to $n_1 = 5, n2 = 3$ when constructing the tensor estimation model, thus the available array aperture of the algorithm poposed in this paper becomes 9, which is greater than the number of array apertures available in the ESPRIT algorithm. From the results shown in the figure, the estimated value of the algorithm poposed in this paper is closer to the true value than the estimated value of the ESPRIT algorithm. The above simulation results well confirm the theoretical analysis, and also show the advantages of multi-target estimation ability brought by the algorithm poposed in this paper by expanding the array aperture.

3.2.1.2 Comparison of estimation performance under different SNR conditions

This experiment mainly tested the RMSE of the angle estimation of the three algorithms when the SNR was changed from -20DB to 20DB. The experimental results are shown in Figure 4.

Figure 4 shows that when the SNR is lower than -15DB, the estimation performance of the ESPRIT algorithm is better than the other two algorithms. When the SNR is greater than -11.3DB, the estimation performance of the algorithm poposed in this paper is better than the other two algorithms. When the SNR is greater than -7.5DB, the estimation performance of the tensor-based algorithm is better than that of the ESPRIT algorithm. This experiment shows that under certain SNR conditions, the denoising ability of the tensor-based DOA estimation algorithm is stronger than that of the ESPRIT algorithm. The algorithm poposed in this paper has further improved the estimation accuracy after expanding the array aperture.

3.2.1.3 Comparison of estimation performance under different number of array elements

This experiment mainly compares and analyzes the estimated performance of the three algorithms when the number of array elements varies from 5 to 45. The experimental results are shown in Figure 5.

Figure 5 shows that when the number of array elements is 5, the tensor-based algorithm produced a larger error. The analysis in 4.1 shows that this is because the available array aperture is 3, which is relatively small compared to the number of targets. When the number of elements is greater than 12, its estimation performance exceeds the ESPRIT algorithm, and when the number of elements is greater than 15, its estimation performance is almost the same as that of the algorithm proposed in this paper. This is because when the ratio of the number of elements to the target number is higher than a certain value, the increase in the number of elements weakened the contribution to the estimation performance. In general, the algorithm proposed in this paper is better than the other two algorithms.

3.2.1.4 Comparison of estimation performance under different number of snapshots
This experiment mainly compares and analyzes the estimated performance of the three algorithms when the number of snapshots varies from 100 to 1000 times. The experimental results are shown in Figure 6.

On the whole, the estimation performance of the three algorithms improves as the number of snapshots increases. The error curve of the algorithm poposed in this paper and the ESPRIT algorithm is better than that of the tensor-based algorithm, while the algorithm poposed in this paper is slightly worse than the ESPRIT algorithm, the reason for this result is also because the information available in the algorithm proposed in this paper only contains the information of 4 array apertures, which is less than the ESPRIT algorithm.

3.2.2 Two-dimensional DOA estimation

Since the algorithm poposed in this paper deals with the two-dimensional DOA estimation problem similarly to the one-dimensional DOA estimation problem, the principles embodied in most of the experimental results are also the same, so this section mainly describes the experimental results without doing too much theoretical analysis.

3.2.2.1 Comparison of estimation performance under different target numbers
This experiment mainly compares and analyzes the RMSE performance of the three algorithms when the number of targets is between 3 and 7. Similar to the one-dimensional DOA estimation, we also conducted targeted experiments on the angle estimation capabilities of 7 targets. The experimental results are shown in Figure 7 to Figure 9.

From Figure 7, the error values of the three algorithms all increase with the increase in the number of targets. The algorithm poposed in this paper is better than the tensor-based algorithm, and the tensor-based algorithm is better than the ESPRIT algorithm. In this experiment, the available array aperture in each dimension of the ESPRIT algorithm and the tensor-based algorithm is 7, while the available array aperture in each dimension of the algorithm poposed in this paper are 13. Note that the information available in each dimension of the algorithm poposed in this paper and the tensor-based algorithm is almost the same as that of the ESPRIT algorithm. Therefore, the performance of the algorithm poposed in this paper and the tensor-based algorithm have been significantly improved compared to the performance of one-dimensional DOA estimation. Especially, when the target number reaches 7, the tensor-based algorithm and the ESPRIT algorithm almost fail, but the algorithm poposed in this paper can still correctly estimate the 7 targets. This can be seen more clearly from Figure 8 and Figure 9 which clearly demonstrated the advantages of the algorithm poposed in this paper.

3.2.2.2 Comparison of estimation performance under different SNR conditions
This experiment compares and analyzes the estimation accuracy of the three algorithms when the SNR varies from -20DB to 20DB. The experimental results are shown in Figure 10. Figure 10 shows that the estimation accuracy of the algorithm poposed in this paper is better than that of the tensor-based algorithm, and the estimation accuracy of the tensor-based algorithm is better than that of the ESPRIT algorithm.

3.2.2.3 Comparison of estimation performance under different number of array elements

This experiment compares and analyzes the estimation accuracy of the three algorithms when the number of array elements varies from 5 to 45. The experimental results are shown in Figure 11. As can be seen from the figure, the estimation accuracy of the algorithm poposed in this paper is better than the other two algorithms under the number of elements. After the number of elements is greater than 7, the estimation accuracy of the ESPRIT algorithm is better than that of the tensor-based algorithm. This shows that in the estimation problem of 3 targets, after the number of elements is greater than 7, the number of elements has a greater impact on the ESPRIT algorithm, and the algorithm poposed in this paper can use more array apertures, so its estimation accuracy is greatly improved. Therefore, its estimation accuracy is still better than the ESPRIT algorithm.

3.2.2.4 Comparison of estimation performance under different number of snapshots

In this experiment, the estimation accuracy of the three algorithms is analyzed and compared when the number of snapshots varies from 10 to 100. The experimental results are shown in Figure 12. It can be seen from the figure that the estimation accuracy of the three algorithms all increase with the increase in the number of snapshots. The estimation accuracy of the algorithm poposed in this paper is higher than that of the tensor-based algorithm, and the estimation accuracy of the tensor-based algorithm is better than that of the ESPRIT algorithm.

4 Conclusions

Under the framework of tensor-based DOA estimation algorithm, this paper proposes an array virtual translation algorithm based on tensor, gives the specific implementation of the algorithm, and applies it to one-dimensional and two-dimensional DOA estimation problems for verification. The simulation results show the feasibility of the algorithm proposed in this paper. In addition, it can be seen from the second section that the algorithm proposed in this paper is simple and easy to use. It is applicable to all tensor-based DOA estimation algorithms under certain conditions. It has strong generalizability and it is of great significance to improve the estimation performance of tensor-based DOA estimation algorithm.

Acknowledgements
Not applicable

Funding
This work was supported by the National Natural Science Foundation of China under Grant 61971438.

Abbreviations
DOA:Direction of arrival
MUSIC:Multiple signal classification
ESPRIT:Estimation of signal parameters via rotational invariance technique
RCS:Reflection cross-sectional area
CPD:canonical polyadic decomposition
HOSVD:Higher-order singular value decomposition
SNR:Signal-to-noise ratio
RMSE:Root mean square error

Availability of data and materials
The datasets used and/or analysed during the current study are available from the corresponding author on reasonable request.

Ethics approval and consent to participate
Not applicable.

Competing interests
The authors declare that they have no competing interests.

Consent for publication
Not applicable.

Authors' contributions
JP completed the writing and computer simulation of the paper, and GZ reviewed the paper and proposed amendments. All authors have read and approved the final manuscript.

Authors' information
Not applicable.

Author details
Air Force Engineering University, Xi'an, China.

References

1. Schmidt, R.: Multiple emitter location and signal parameter estimation. IEEE Transactions on Antennas and Propagation **34**, 276–280 (1986)
2. Roy, R., Kailath, T.: Esprit-estimation of signal parameters via rotational invariance techniques. IEEE Transactions on Acoustics, Speech, and Signal Processing **37**, 984–995 (1989)
3. Shan, T.-J., Wax, M., Kailath, T.: On spatial smoothing for direction-of-arrival estimation of coherent signals. IEEE Transactions on Acoustics, Speech, and Signal Processing **33**, 806–811 (1985)
4. Pillai, S.U., Kwon, B.H.: Forward/backward spatial smoothing techniques for coherent signal identification. IEEE Transactions on Acoustics, Speech, and Signal Processing **37**, 8–15 (1989)
5. Chen, Y.-M.: On spatial smoothing for two-dimensional direction-of-arrival estimation of coherent signals. IEEE Transactions on Signal Processing **45**, 1689–1696 (1997)
6. Peng, J., Zheng, G., Zhu, Q.: A novel weighted spatial smoothing doa estimation algorithm for coherent signals. In: 2020 IEEE 3rd International Conference on Electronic Information and Communication Technology (ICEICT), pp. 504–508 (2020)
7. Bohme, J.: Estimation of source parameters by maximum likelihood and nonlinear regression. In: ICASSP '84. IEEE International Conference on Acoustics, Speech, and Signal Processing, pp. 271–274 (1984)
8. Stoica, P., Ottersten, B., Viberg, M., Moses, R.L.: Maximum likelihood array processing for stochastic coherent sources. IEEE Transactions on Signal Processing **44**, 96–105 (1996)
9. Bhaskar, B.N., Tang, G., Recht, B.: Atomic norm denoising with applications to line spectral estimation. IEEE Transactions on Signal Processing **61**, 5987–5999 (2013)
10. Chen, Y., Chi, Y.: Robust spectral compressed sensing via structured matrix completion. IEEE Transactions on Information Theory **60**, 6576–6601 (2014)
11. Chi, Y., Chen, Y.: Compressive two-dimensional harmonic retrieval via atomic norm minimization. IEEE Transactions on Signal Processing **63**, 1030–1042 (2015)
12. Yang, Z., Xie, L.: Enhancing sparsity and resolution via reweighted atomic norm minimization. IEEE Transactions on Signal Processing **64**, 995–1006 (2016)
13. Zhang, Z., Wang, Y., Tian, Z.: Efficient two-dimensional line spectrum estimation based on decoupled atomic norm minimization. Signal Processing **163**, 95–106 (2019)
14. Nion, D., Sidiropoulos, N.D.: Tensor algebra and multidimensional harmonic retrieval in signal processing for mimo radar. IEEE Transactions on Signal Processing **58**, 5693–5705 (2010)
15. Papy, J.M., De Lathauwer, L., Van Huffel, S.: Exponential data fitting using multilinear algebra: the single-channel and multi-channel case. Numerical Linear Algebra with Applications **12**, 809–826 (2005)
16. Thakre, A., Haardt, M., Roemer, F., Giridhar, K.: Tensor-based spatial smoothing (tb-ss) using multiple snapshots. IEEE Transactions on Signal Processing **58**, 2715–2728 (2010)
17. Xu, F., Vorobyov, S.A., Yang, X.: Joint dod and doa estimation in slow-time mimo radar via parafac decomposition. IEEE Signal Processing Letters **27**, 1495–1499 (2020)
18. Wen, F., Shi, J., Zhang, Z.: Joint 2d-dod, 2d-doa, and polarization angles estimation for bistatic emvs-mimo radar via parafac analysis. IEEE Transactions on Vehicular Technology **69**, 1626–1638 (2020)
19. Shi, J., Wen, F., Liu, T.: Nested mimo radar: Coarrays, tensor modeling, and angle estimation. IEEE Transactions on Aerospace and Electronic Systems **57**, 573–585 (2021)
20. Zheng, H., Zhou, C., Gu, Y., Shi, Z.: Two-dimensional doa estimation for coprime planar array: A coarray tensor-based solution. In: ICASSP 2020 - 2020 IEEE International Conference on Acoustics, Speech and Signal Processing (ICASSP), pp. 4562–4566 (2020)
21. Kolda, T.G., Bader, B.W.: Tensor decompositions and applications. SIAM Review **51**, 455–500 (2009)
22. Cichocki, A., Mandic, D., De Lathauwer, L., Zhou, G., Zhao, Q., Caiafa, C., PHAN, H.A.: Tensor decompositions for signal processing applications: From two-way to multiway component analysis. IEEE Signal Processing Magazine **32**, 145–163 (2015)
23. Sidiropoulos, N.D., De Lathauwer, L., Fu, X., Huang, K., Papalexakis, E.E., Faloutsos, C.: Tensor decomposition for signal processing and machine learning. IEEE Transactions on Signal Processing **65**, 3551–3582 (2017)
24. Vervliet, N. and Debals, O. and Sorber, L. and Van Barel, M. and De Lathauwer, L.: Tensorlab 3.0 (2016). https://www.tensorlab.com/ Accessed Accessed 25 Feb 2021

Table 1 Numerical simulation parameter setting

	One-dimensional DOA estimation	Two-dimensional DOA estimation
Monte Carlo simulation times	20	20
Number of array elements	N=7	N=7,M=7
Number of targets	K=3	K=3
Signal-to-noise ratio	SNR=10	SNR=10
Snapshots	L=100	L=100

Figures
Tables
Additional Files
Additional file 1 — Sample additional file title
Additional file descriptions text (including details of how to view the file, if it is in a non-standard format or the file extension). This might refer to a multi-page table or a figure.

Additional file 2 — Sample additional file title
Additional file descriptions text.

Figures

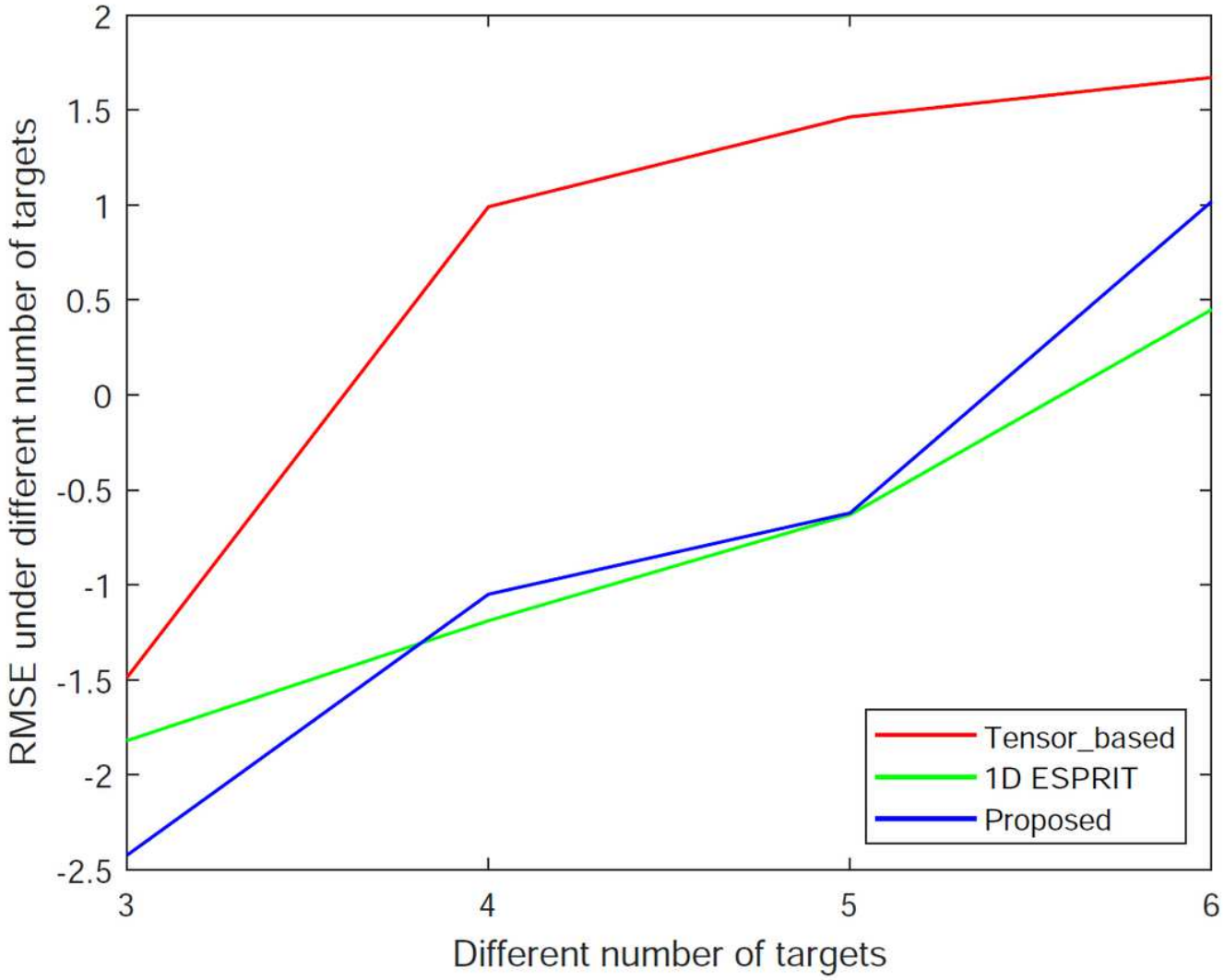

Figure 1

shows that the RMSE of the three algorithms increases with the increase of the number of targets. And the error curve of the algorithm poposed in this paper and the ESPRIT algorithm is better than that of the tensor-based algorithm because the available array aperture of the tensor-based algorithm is relatively small.

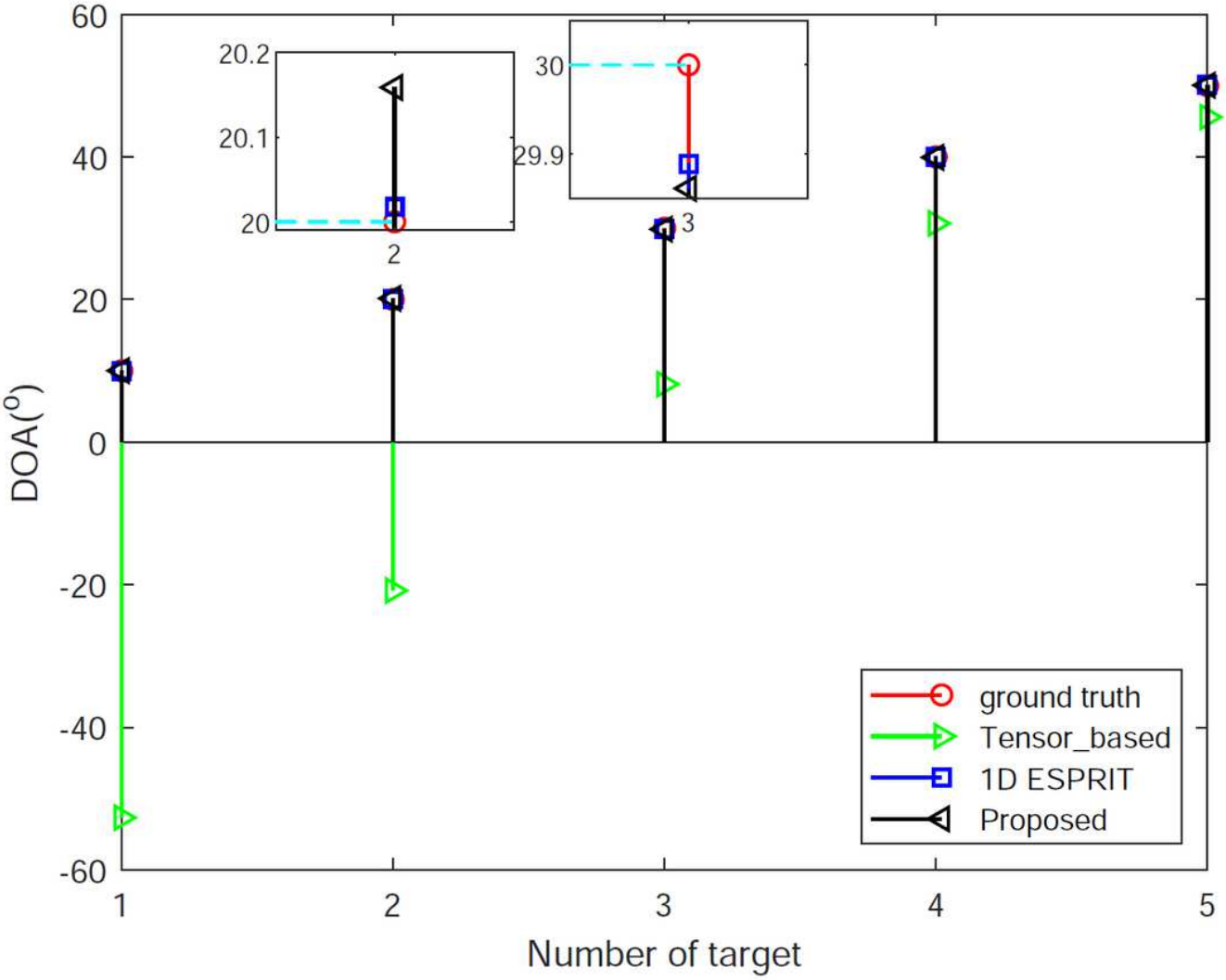

Figure 2

shows that the tensor-based algorithm completely fails when estimating the 5 targets, and the estimation accuracy of the algorithm poposed in this paper is lower than that of the ESPRIT algorithm.

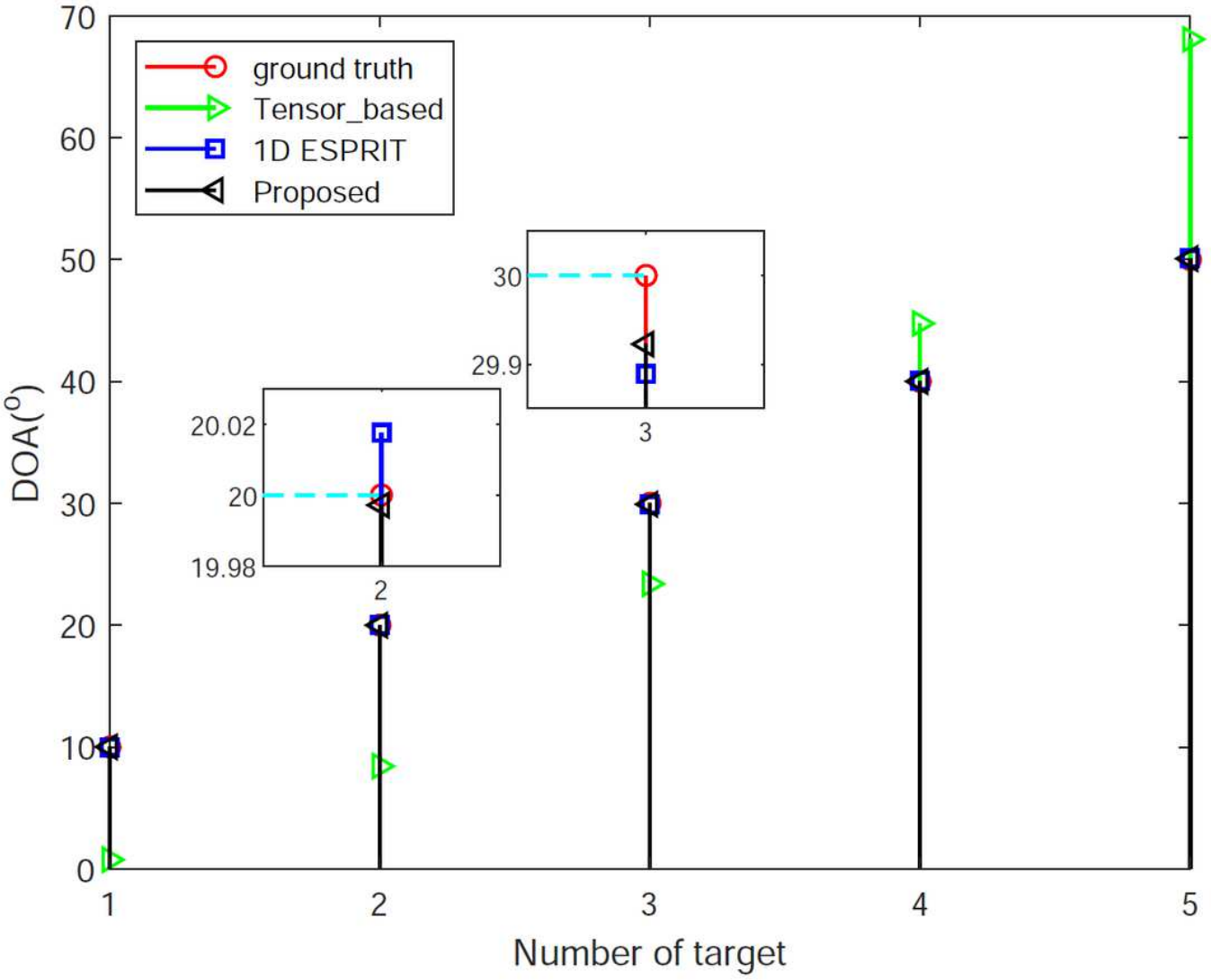

Figure 3

In order to verify that the algorithm poposed in this paper can make up for this deficiency by expanding the aperture of the array, in the experiment shown in Figure 3,

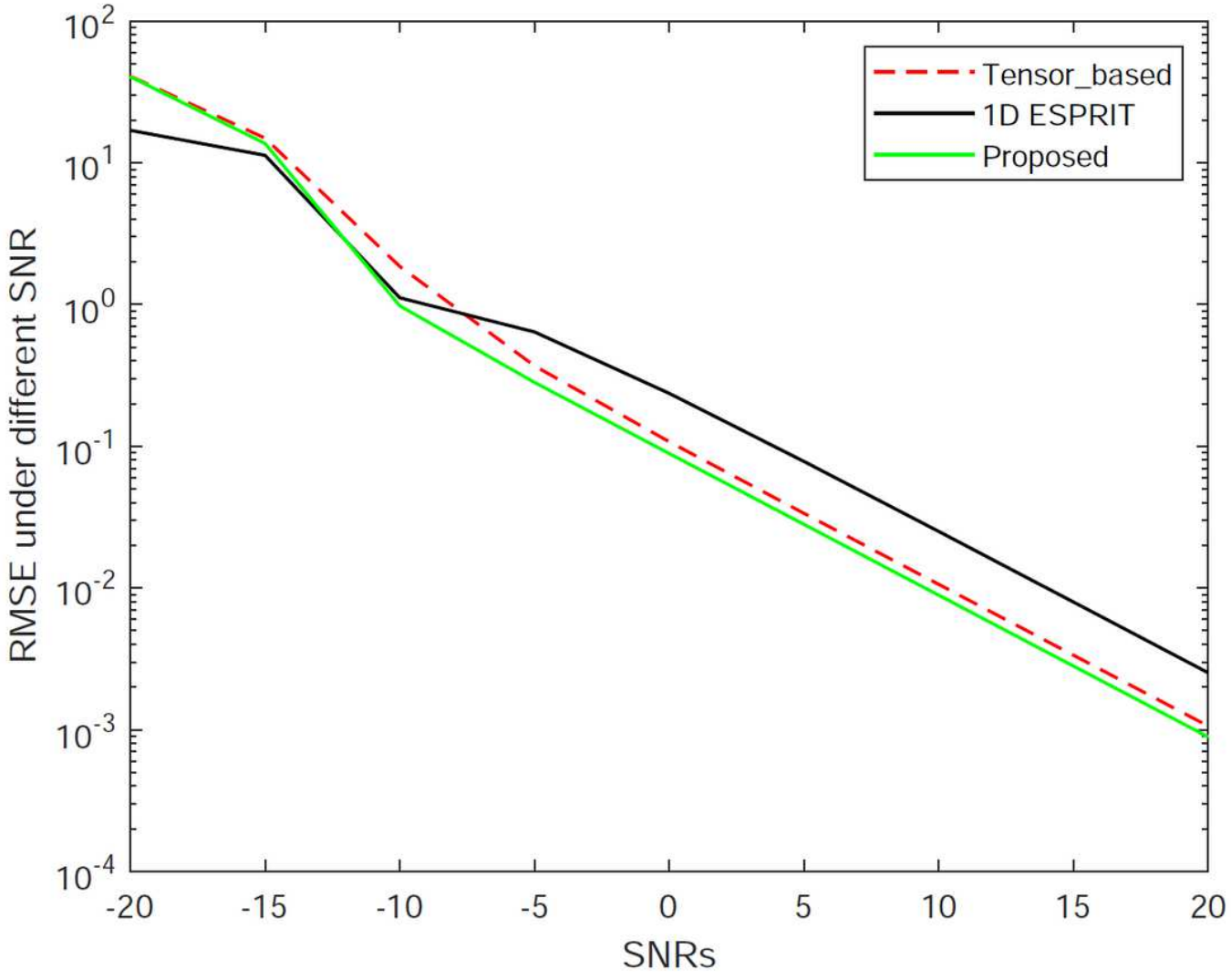

Figure 4

shows that when the SNR is lower than -15DB, the estimation performance of the ESPRIT algorithm is better than the other two algorithms.

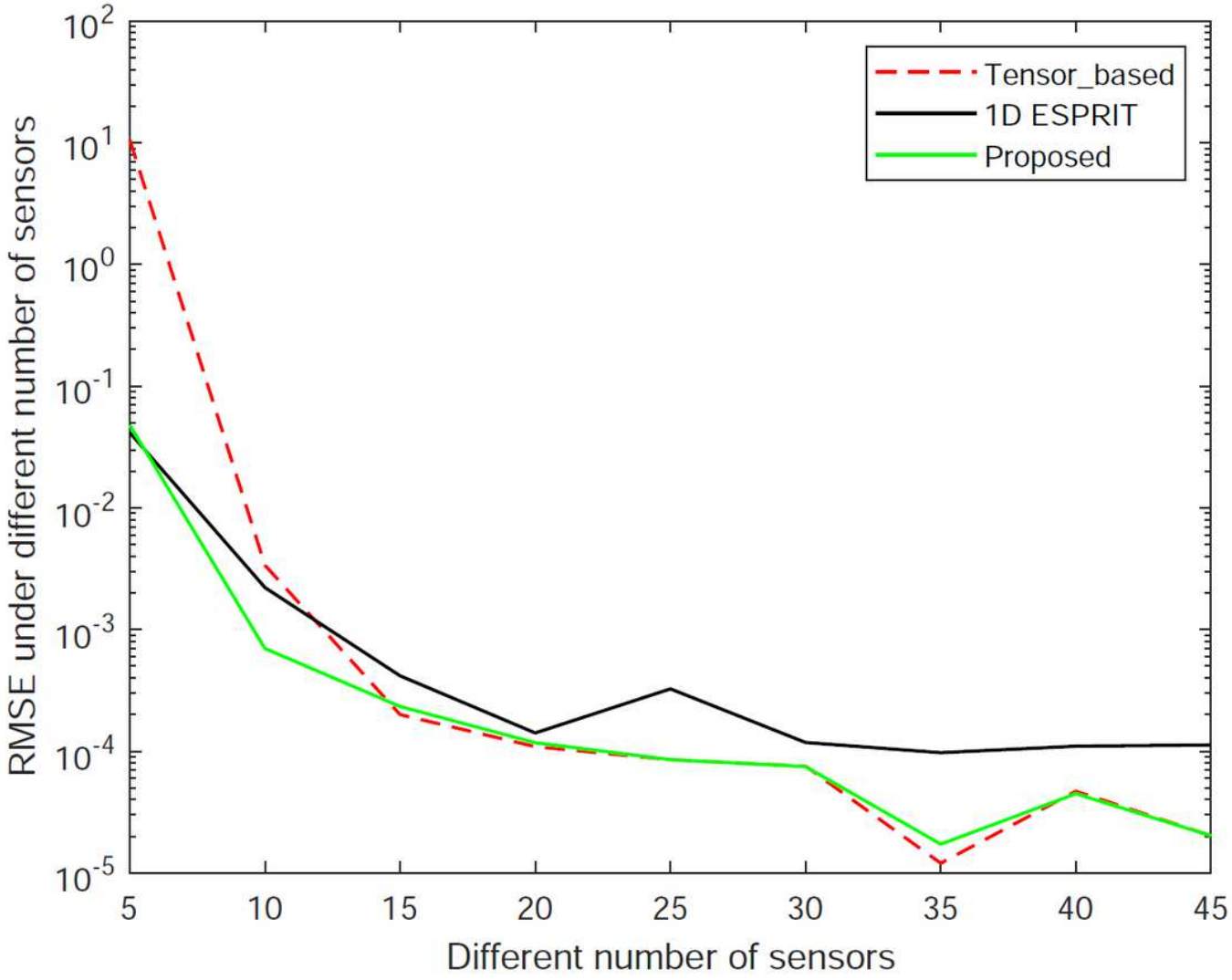

Figure 5

shows that when the number of array elements is 5, the tensor-based algorithm produced a larger error.

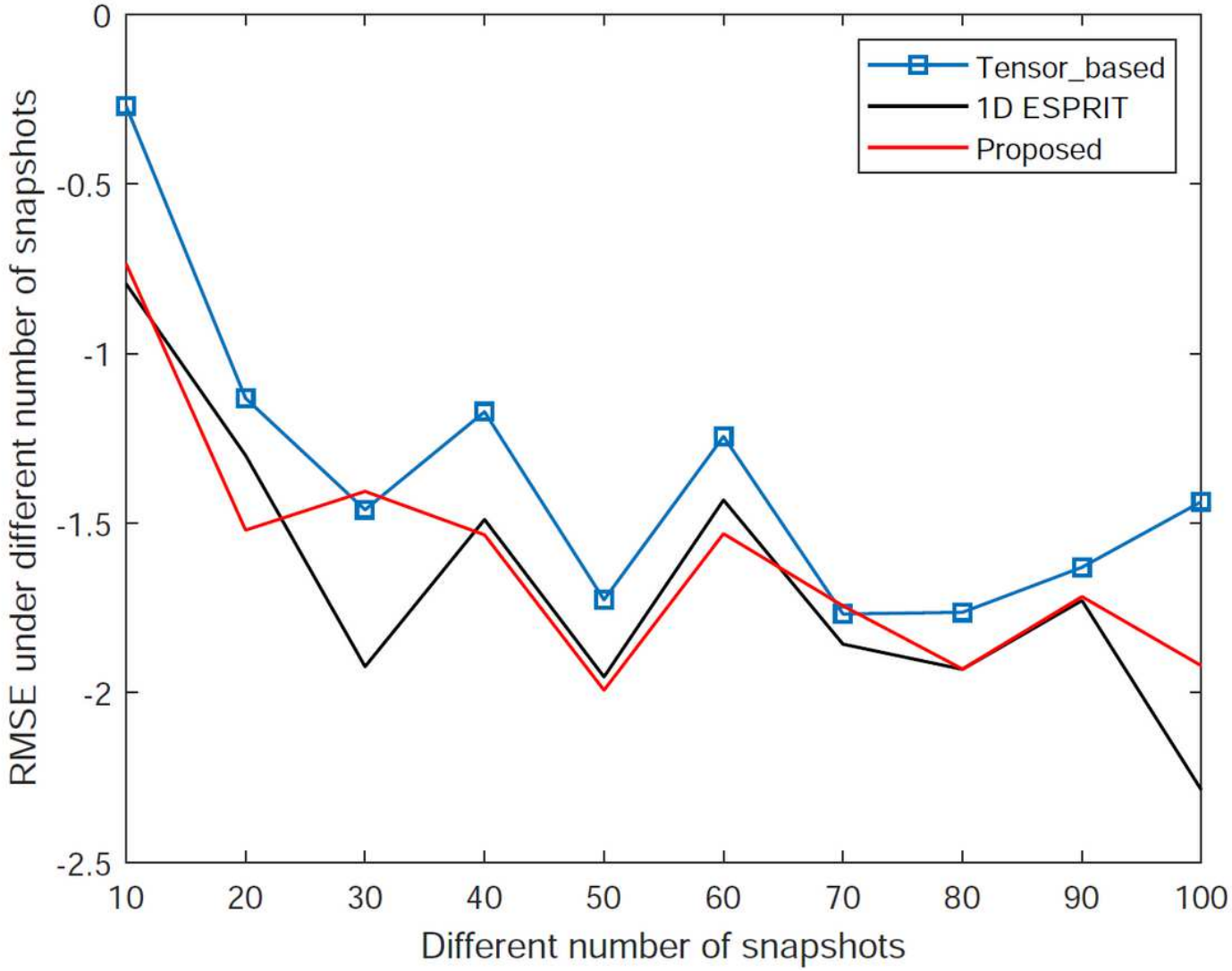

Figure 6

The experimental results are shown in Figure 6. On the whole, the estimation performance of the three algorithms improves as the number of snapshots increases.

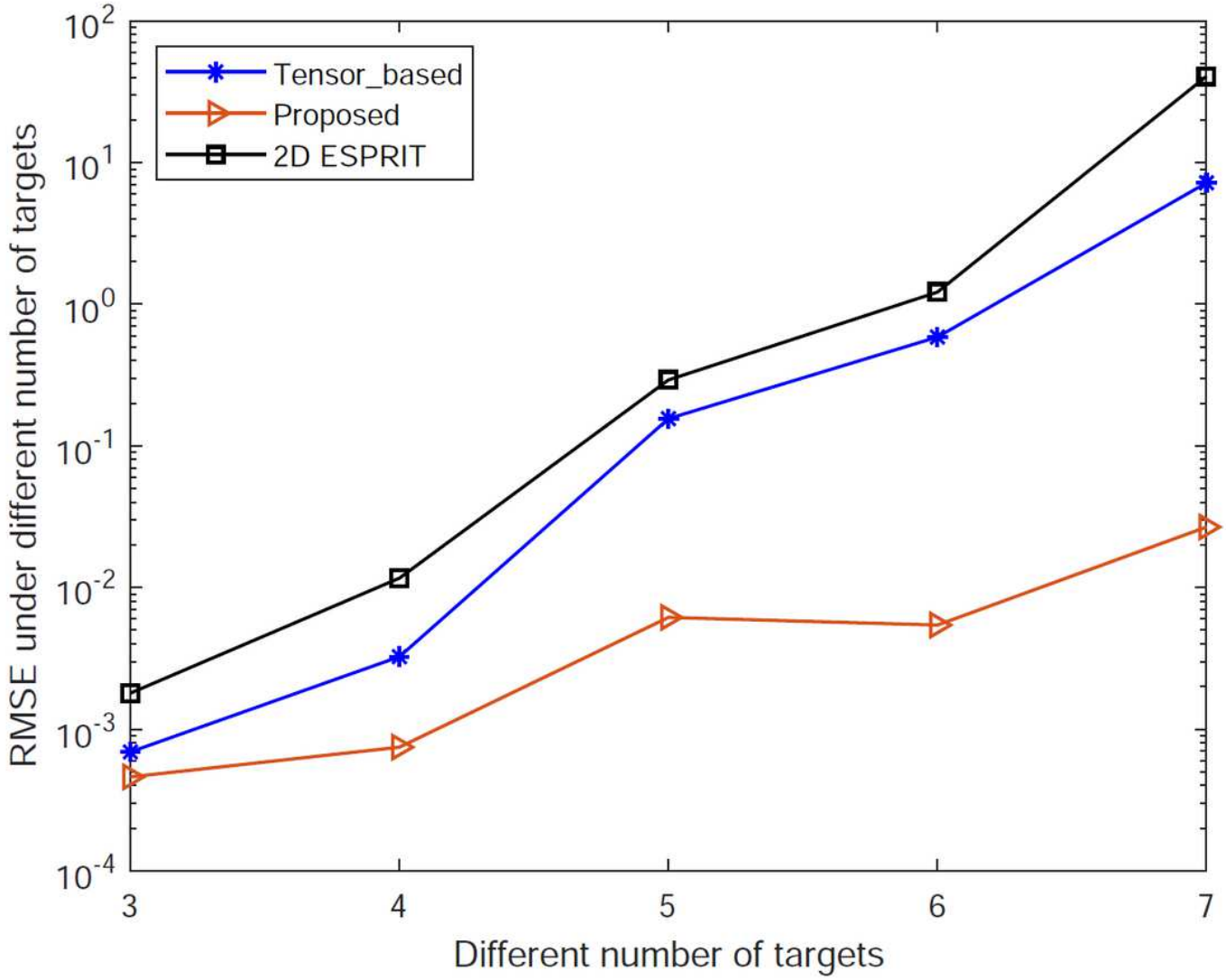

Figure 7

the error values of the three algorithms all increase with the increase in the number of targets.

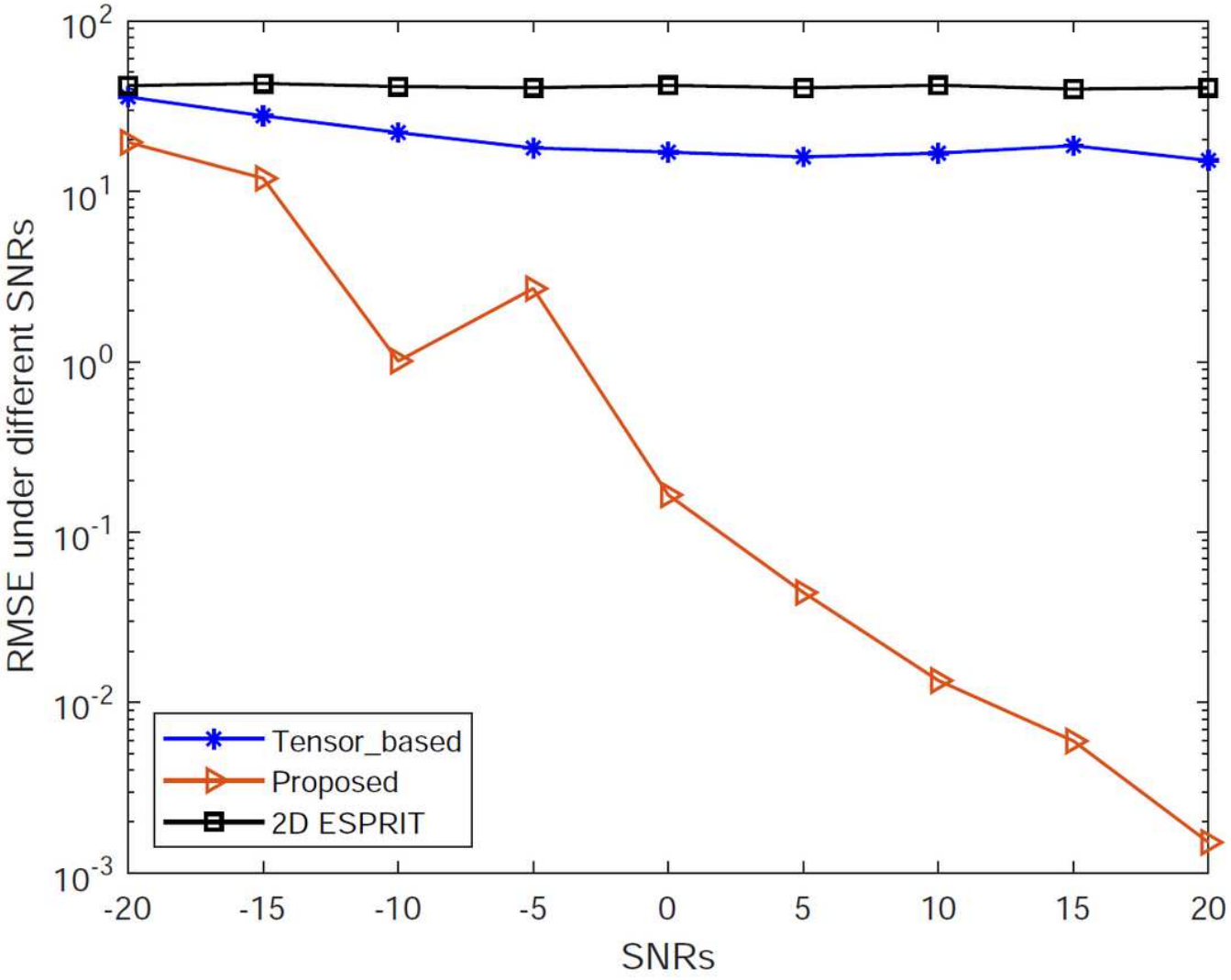

Figure 8

which clearly demonstrated the advantages of the algorithm poposed in this paper.

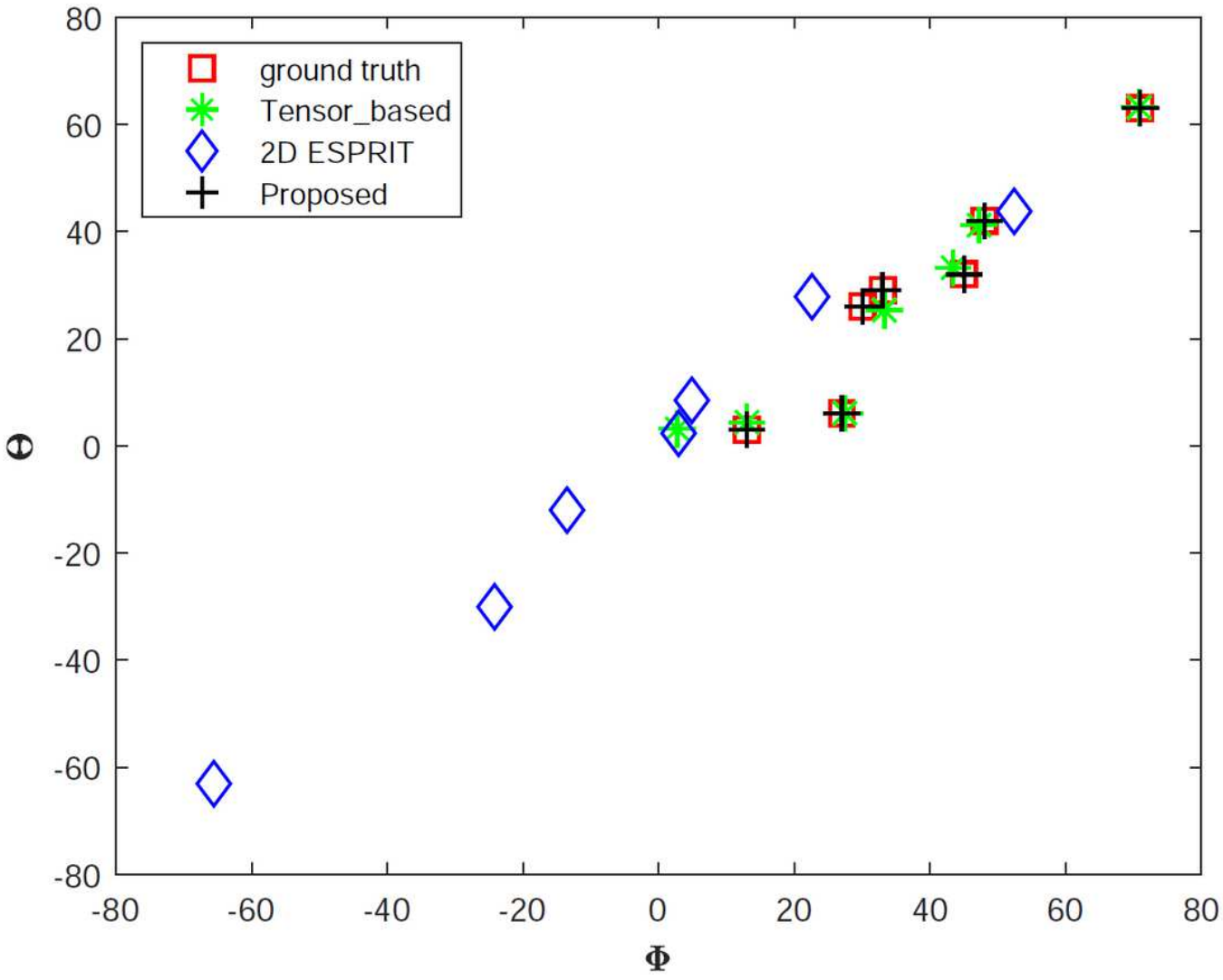

Figure 9

which clearly demonstrated the advantages of the algorithm poposed in this paper.

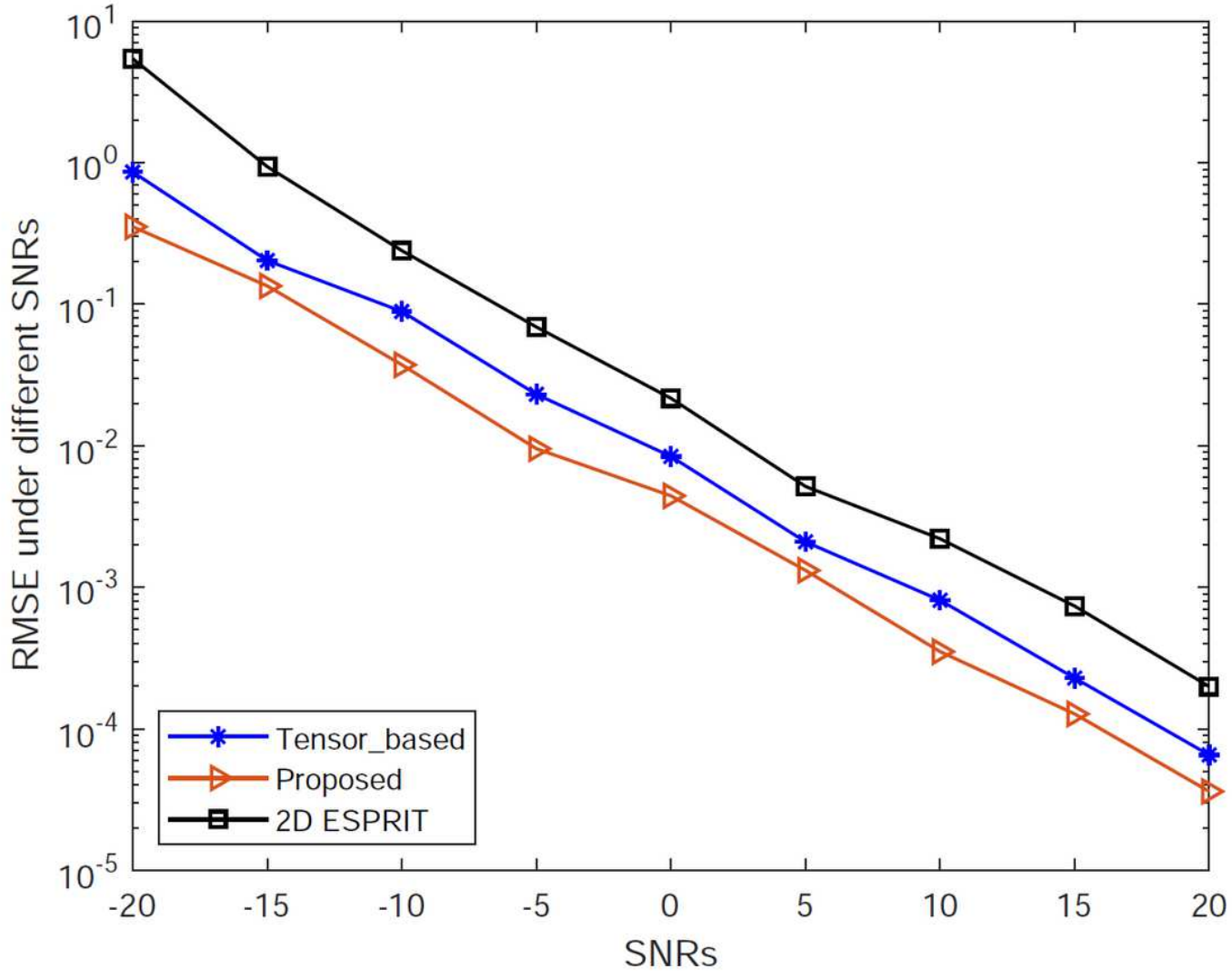

Figure 10

shows that the estimation accuracy of the algorithm poposed in this paper is better than that of the tensor-based algorithm, and the estimation accuracy of the tensor-based algorithm is better than that of the ESPRIT algorithm

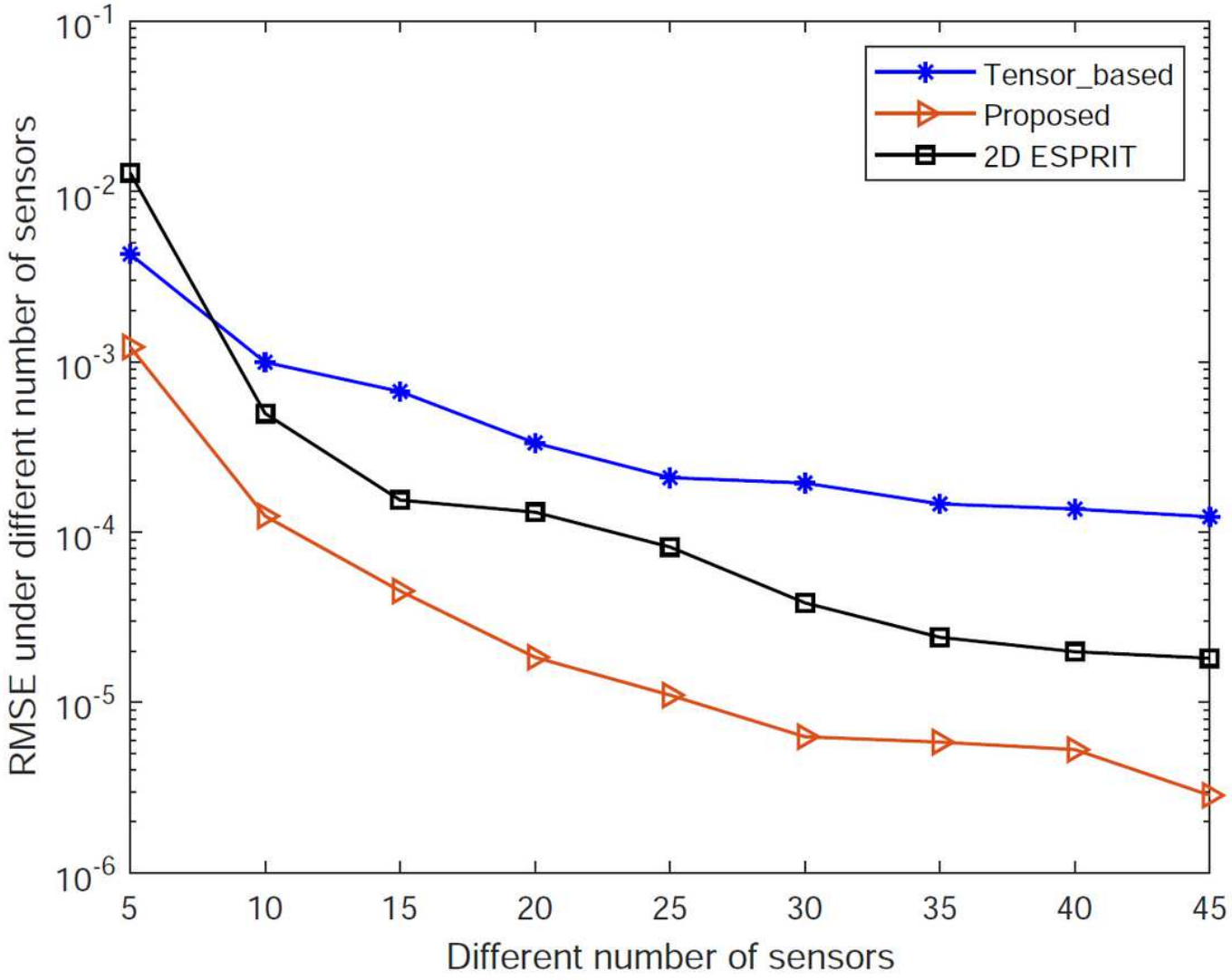

Figure 11

The experimental results are shown in Figure 11. As can be seen from the figure, the estimation accuracy of the algorithm poposed in this paper is better than the other two algorithms under the number of elements.

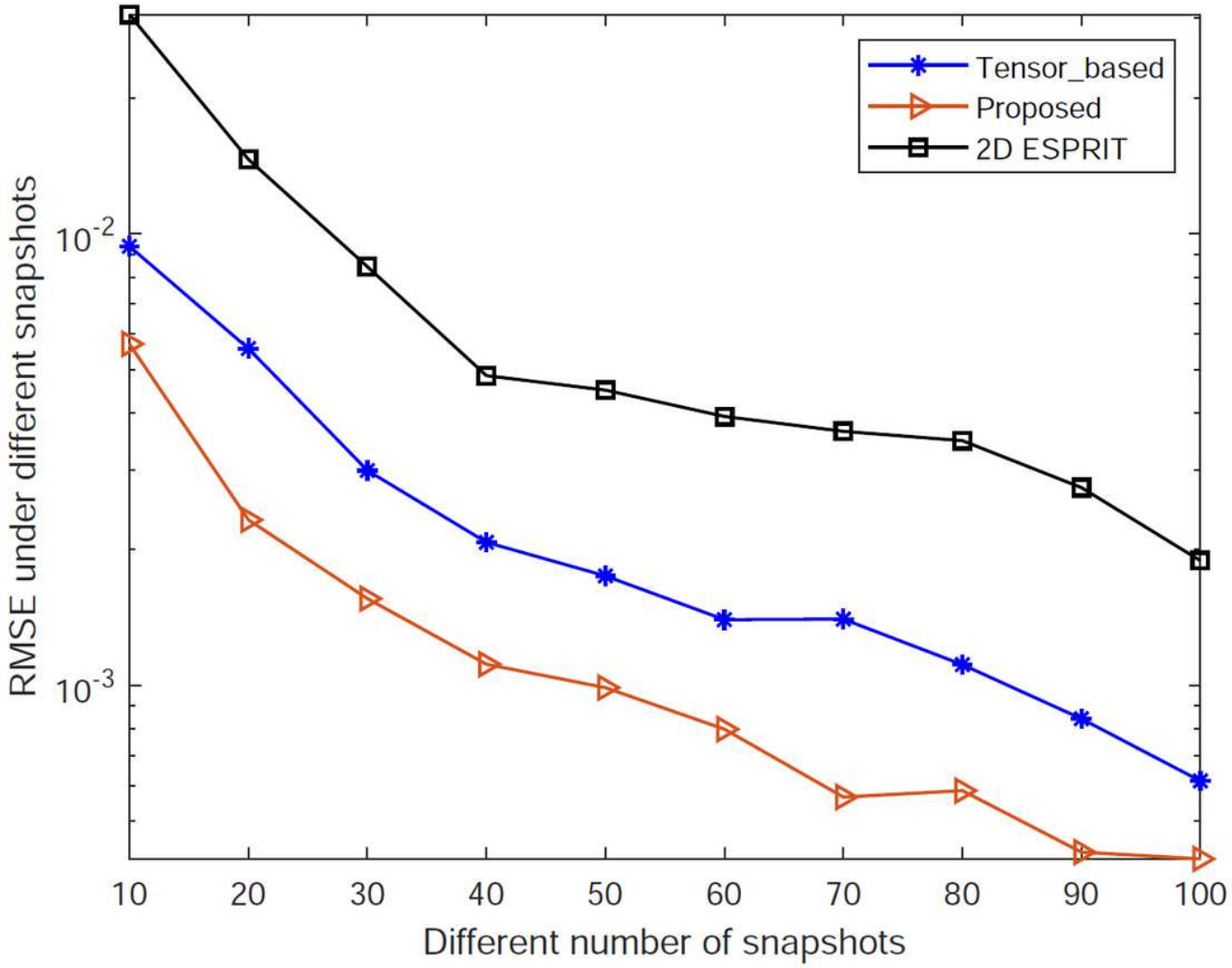

Figure 12

The experimental results are shown in Figure 12. It can be seen from the figure that the estimation accuracy of the three algorithms all increase with the increase in the number of snapshots.